ADVANCED FUNCTIONAL MATERIALS
www.afm-journal.de

Graphene at the Atomic-Scale: Synthesis, Characterization, and Modification

*Erin V. Iski, Esmeralda N. Yitamben, Li Gao, and Nathan P. Guisinger**

Graphene is nature's ideal two-dimensional conductor and is comprised of a single sheet of hexagonally packed carbon atoms. Since the first electrical measurements made on graphene, researchers have been trying to exploit the unique properties of this material for a variety of applications that span numerous scientific and engineering disciplines. In order to fully realize the potential of graphene, large scale synthesis of high quality graphene and the ability to control the electronic properties of this material on a nanometer length-scale are necessary and remain key challenges. This article will review the efforts at the Center for Nanoscale Materials that focus on the atomic-scale characterization and modification of graphene via scanning tunneling microscopy and its synthesis on various materials (SiC, Cu(111), Cu foil, etc.). These fundamental studies explore growth dynamics, film quality, and the role of defects. The chemical modification of graphene following exposure to atomic hydrogen will also be covered, while additional emphasis will be made on graphene's unique structural properties.

1. Introduction

Since the first experimental isolation of a single sheet less than a decade ago,[1–3] graphene has become one of the most studied systems in modern materials science as well as several other scientific disciplines. There are several physical and chemical properties that make this material extremely attractive and promising for a wide range of both fundamental and applied applications. It is a sheet of hexagonally packed carbon atoms that are sp^2 bonded, and this sheet is only one atom thick, as illustrated in the schematic of **Figure 1** a. Graphene is one of carbon's many allotropes, like diamond etc. Bernal stacking of graphene results in a three-dimensional graphite crystal, while rolling graphene into a cylinder gives the structure of a one-dimensional carbon nanotube. Graphene itself is an ideal two-dimensional material. As a relatively new material system, the initial efforts by numerous scientists have helped to overcome many obstacles related to characterization, synthesis, and processing while at the same time expanding graphene's potential and introducing a new set of challenges.

The first material challenge was isolating a single sheet of graphene, which was accomplished through mechanical exfoliation from a graphite crystal.[1–3] This simple technique has made the experimental investigation of graphene accessible to almost any interested research group regardless of scientific discipline or available resources. The only drawback is that mechanical exfoliation is not scalable beyond one small flake of graphene. However, significant advances have been made in the scalable synthesis of large-area graphene sheets. The two main forms of large-scale synthesis involve the thermal decomposition of silicon carbide or CVD (chemical vapor deposition) growth, i.e., the thermal decomposition of hydrocarbons on transition metals, as illustrated in Figure 1b. The synthesis and characterization of these two processes will be discussed in more detail in the next section. The two-dimensional nature of graphene makes this material extremely compatible with existing planar processing techniques. One of the main challenges still remaining is the quality of the graphene that results from large-scale synthesis techniques.

Of its numerous exciting properties, the one material property that stands out is graphene's very unique band structure. It is a zero-gap material whose band structure is linear at low energies, resulting in massless carriers that behave relativistically and are defined by the Dirac equation. Combined with symmetry and scattering rules, the carriers (electrons and holes) have long coherence lengths that for practical applications result in extremely high mobilities. This article will not delve deep into the rich fundamental physics of graphene, which have been well described in several other reviews.[4,5] The zero-gap around the Dirac point makes it very easy to electrostatically gate graphene and change the carriers from electrons to holes. On the other hand, this same property makes it very difficult to turn transport off when trying to mimic a conventional switch or transistor. As a result, many efforts are underway to create a controlled bandgap in graphene, which

Dr. E. V. Iski, Dr. E. N. Yitamben
Center for Nanoscale Materials
Argonne, IL 60439, USA
Prof. L. Gao
Department of Physics
California State University
Northridge, CA 91330, USA
Dr. N. P. Guisinger
Argonne National Laboratory
9700 S. Cass Ave Bldg. 440, Lemont, IL 60439, USA
E-mail: nguisinger@anl.gob

DOI: 10.1002/adfm.201203421

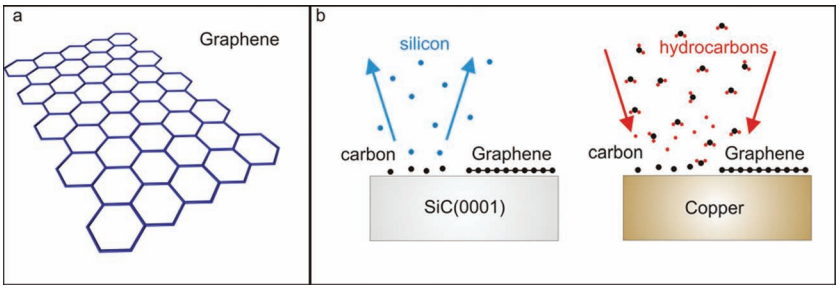

Figure 1. Schematic illustration of graphene synthesis. a) Schematic model of graphene showing the hexagonal arrangement of a one atom thick sheet. b) Two different types of large scale synthesis. The schematic on the left represents the thermal decomposition of SiC when heated to 1250 °C. The schematic on the right depicts CVD growth on heated transition metals (in this case copper).

can be done through size confinement (nanoribbons) or chemical modification.[6–11] The latter is hampered by the chemical inertness of the material. Graphene is very chemically robust allowing it to maintain its material integrity through conventional planar processing. Graphene also has an extremely high coefficient of thermal conductivity,[12,13] which can be extremely beneficial due to the challenges of thermal management in conventional electronics.

The sheer range of material properties attributed to graphene has enabled graphene studies to extend beyond the potential advancement of conventional transport devices. Graphene is also biologically compatible and is being utilized as a cell support with several sensing applications.[14–16] A single sheet is over 90% transparent and several studies are utilizing graphene as an advanced transparent conductor.[17,18] Others are utilizing graphene in fuel cells,[19] catalysis,[20] and lithium ion technologies.[21] As will be discussed later in the article, graphene is also an impenetrable membrane, even to atomic hydrogen, which introduces other potential applications such as corrosion resistance. Suspended graphene is being explored as a mechanical resonator,[22,23] as well as a membrane to encapsulate chemical reactions.[24] In almost all of these studies and applications, the one universal challenge is the ability to precisely engineer and control graphene's unique material properties.

Scanning tunneling microscopy (STM) and spectroscopy (STS) have been invaluable tools for characterizing the structural, chemical, electrical, and even magnetic properties of graphene.[25–28] This article will review aspects of graphene synthesis and modification and our role in the characterization of graphene at the atomic-scale. The main synthesis focus will be on CVD growth on both single crystal Cu(111) and polycrystalline Cu foil. These studies helped to identify defects and domain boundaries and their role in significantly reducing graphene's electrical mobility. The growth of graphene on SiC(0001) was utilized as a template for hydrogen modification and molecular self-assembly. The hydrogen saturation of graphene results in an altering of its electronic properties making it insulating by opening a bandgap. Furthermore, graphene is found to act as a shielding layer between physisorbed molecules and the underlying substrates. These topics will be discussed in detail in the following sections which review the STM efforts at the Center for Nanoscale Materials (CNM) to characterize the synthesis and chemical modification of graphene. All of these studies were performed with commercial and homebuilt instruments that are within an ultrahigh vacuum environment and are part the CNM's User Program.

2. Synthesis and Characterization

2.1. Epitaxial Growth on SiC(0001)

The first studies of graphite formation on 6H-SiC(0001) demonstrated that a carbon rich surface could be formed through the sublimation of Si by heating the C-face or Si-face in ultrahigh vacuum (UHV) at temperatures ranging from 1000 to 1500 °C.[29] The resulting carbon layers have a graphene-like structure with sp^2 bonding, which is in alignment with the SiC substrate.[29–40] Importantly, the growth of graphene on the two different faces, C or Si, is substantially different in terms of the growth kinetics with the growth on the C-face occurring much faster than on the Si-face.[29,31,33–35] Also, the graphene grown on the Si-face is epitaxial with a 30° rotation of the carbon atomic lattice relative to the SiC lattice, while the films on the C-face show a variety of phases with different orientations.[29,35] Much of the experimental and theoretical studies have focused on the Si-face growth, due to the variety in orientations on the C-face, however, it also been shown that the quality of C-face graphene may be superior to that of Si-face graphene.[41] Conversely, multilayers films with an azimuthal disorder between the different layers have also been observed when growing on the C-face.[42,43] Overall, graphene grown on SiC by in situ heating consisted of small flakes with an inhomogeneous graphene thickness.[44] Similar to some of the graphene growth on metal surfaces, it is possible to use an inductively heated furnace to grow graphene on SiC with different research groups using slightly different recipes. One group used isothermal conditions at 2000 °C with an ambient argon pressure of 1 atm.[45] Another group used the same ambient gas, but went to 1650 °C;[46] while, a third group used disilane as the ambient gas and went to a range of temperatures from 800 to 1300 °C.[47]

There is some minor confusion and/or debate over the transition from the SiC surface reconstruction to a single sheet of graphene and on to thicker layers. When the SiC is heated in UHV the process begins with Si sublimating from the surface. Prior to graphitization, the surface undergoes several different surface reconstructions as a function of Si depletion, which has been well documented via STM studies.[30,45] This depletion is not only from the first layer but involves multiple layers. The final reconstruction before graphene synthesis seems to be a $(6\sqrt{3} \times 6\sqrt{3})R30°$ surface reconstruction, which is very complicated because of its large unit cell and is comprised of multiple layers before reaching the bulk. The STM images of **Figure 2**a,b show the transition from the graphene "buffer" layer to the $(6\sqrt{3} \times 6\sqrt{3})R30°$ SiC surface reconstruction. The "buffer" layer is the graphene sheet closest to the SiC substrate, as illustrated in Figure 2c. Although it is structurally and chemically

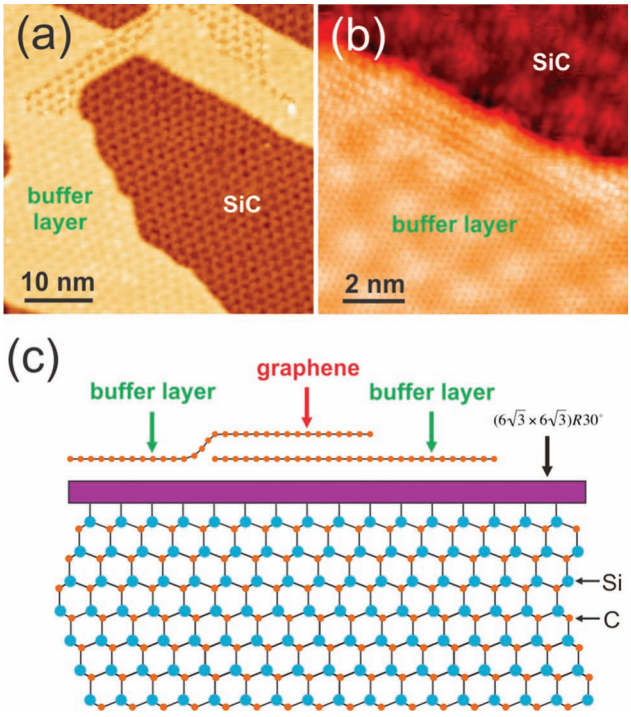

Figure 2. Atomic-scale characterization of epitaxial graphene on SiC(0001). a) This STM image shows regions of exposed $(6\sqrt{3} \times 6\sqrt{3})$ R30° SiC surface reconstruction and epitaxial graphene labeled as the "buffer" layer. (Imaging conditions: I = 100 pA, V = 1.5 V). b) Atomic resolution image showing the transition from the graphene "buffer" layer to the SiC surface reconstruction. (Imaging conditions: I = 100 pA, V = 0.5 V). c) Schematic illustration to clarify our nomenclature of a "buffer" layer of graphene vs. the $(6\sqrt{3} \times 6\sqrt{3})$R30° reconstruction.

identical, we distinguish this layer from the thicker graphene layers, because this sheet is electronically different due to a strong interaction with the substrate. The confusion lies in the fact that some argue there is an invisible graphene sheet above the area we label as $(6\sqrt{3} \times 6\sqrt{3})$R30°, and they name this invisible region as the "buffer" layer. We do not dispute this interpretation, but it is not supported by the STM experiments. We can resolve the atoms within the $(6\sqrt{3} \times 6\sqrt{3})$R30° region and would easily resolve any additional atomic structure. Furthermore, the area that we identify as the $(6\sqrt{3} \times 6\sqrt{3})$R30° SiC surface reconstruction is structurally, chemically, and electronically different from any of the graphene regions. Regions of the $(6\sqrt{3} \times 6\sqrt{3})$R30° reconstruction are much more reactive and will saturate with atomic hydrogen before any is detected on the graphene. As you will see at the end of the review, the ordering of physisorbed molecules is strongly affected by this region as well.

2.2. CVD on Transition Metals

The use of CVD achieved through the high temperature decomposition of various hydrocarbon sources to produce thin, graphitic layers on transition metal surfaces and metal carbides have been studied for over 40 years.[46–48] The CVD growth process involves the thermal decomposition of a hydrocarbon source on a heated substrate. Depending on the substrate, the process can be catalytically enhanced. In most cases, the carbon will diffuse/dissolve into the heated substrate according to the carbon solubility of the transition metal. As the substrate cools, the dissolved carbon will segregate to the surface to form sheets of graphene. For most transition metals, the ability to control the thickness of the graphene layers and the uniformity of the sheets are the main challenges to the formation of pristine graphene. These techniques have been perfected over time as the early experiments resulted in thick graphitic crystals instead of the currently desired graphene films. Improvements to the technique include using thin films of transition metals on SiO_2/Si substrates and subsequently growing the graphene in quartz tubes contained within high temperature furnaces under an argon atmosphere.[49] Importantly, this type of growth procedure allows fine control over the amount of graphene grown as it possible to subtly change the growth parameters, like temperature and the amount of reactive gases that are used as precursors and reactants in the deposition process. Furthermore, CVD growth of graphene has been extended to a variety of metals and has been thoroughly outlined in a recent and excellent review by Matthias Batzill.[50]

One of the more relevant systems for graphene growth in the recent years has been on polycrystalline Cu foil and subsequently on Cu single crystals.[18,51–60] The growth mode of these systems is dictated by the low carbon solubility on Cu, which facilitates the formation of graphene platelets that ultimately coalesce to form a complete film and also leads to self-limiting growth of a single monolayer. Polycrystalline Cu foil, an amenable substrate for industry and/or scale-up opportunities, was shown to be an excellent substrate for the CVD growth of graphene.[51] The authors were able to grow large-area graphene films on the order of centimeters on copper foil substrates using the decomposition of methane. Throughout the recent literature, the quality of the films on Cu foil has been verified with continuous growth over Cu surface steps and grain boundaries and with the determination that the amount of multi-layer regions of graphene comprises a very small overall percentage.[50,61–70] Importantly, the electronic structure of graphene on Cu closely resembles that of free standing graphene, furthering the exploration of graphene on this substrate.[50] With that being said, it was also discovered that CVD-grown graphene had a lower mobility, greater impurity doping, and higher asymmetry among electron and hole conduction.[51,53,71–75] Initially, it was postulated that possibly the low mobility was due to the etching or chemical contamination of graphene during the transfer process.[49,51,71,72,76,77]

The epitaxial growth of graphene on a Cu(111) single crystal was originally devised as a mechanism to further understand the reduction in mobility of charge carriers in graphene grown on Cu foil and as a fundamental study of graphene morphology.[54] The graphene growth on the crystal was accomplished through thermal decomposition of ethylene in an ultrahigh vacuum system. Using STM and STS to characterize both the morphology and electrical properties, respectively, the authors were able to study how the nucleation of monolayer islands with two different domain orientations led to the formation of numerous domain boundaries with increasing

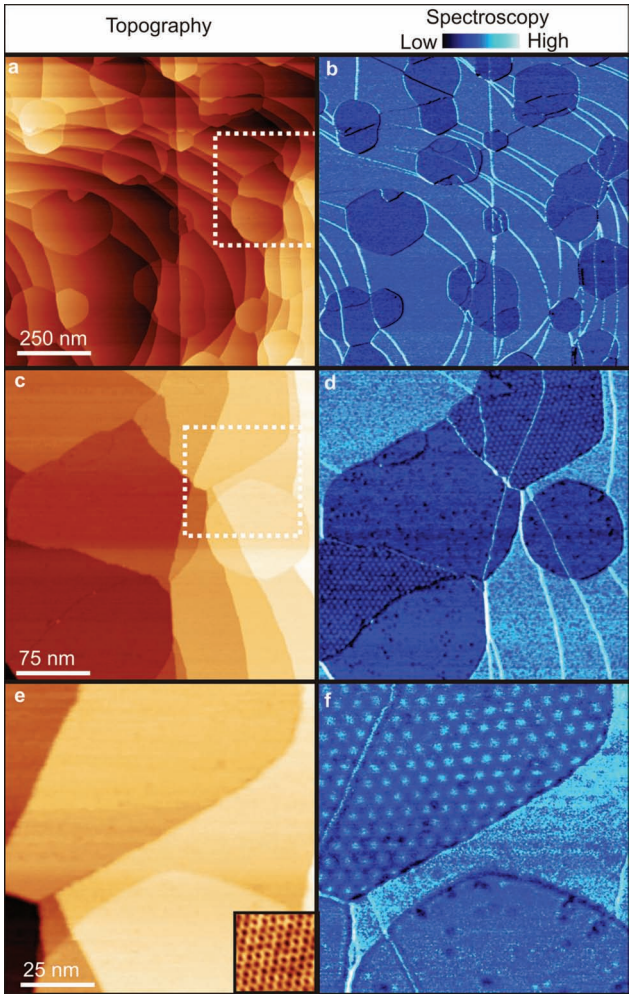

Figure 3. Series of STM topography and differential conductance (*dI/dV*) images of graphene islands grown on Cu(111). a) Large-scale topography image showing the graphene islands (0.35 ML) on the copper surface, demonstrating how the domains are spotted across the metal surface and are not part of one domain. b) Corresponding dI/dV map of the same area in (a) indicating the electrical contrast of the graphene islands relative to the copper and emphasizing the continuous growth over step edges. c) Zoomed-in topographic image from the white, dotted box in (a). d) A differential conductance image of the same area in (c) can be used to see the emerging Moiré pattern of those areas of copper which are covered with graphene. e) Small-scale STM image of the area from the white, dotted box in (c), where the inset shows the Moiré pattern of the graphene within that region. f) Simultaneously derived *dI/dV* image of the area in (e), clearly indicating the honeycomb structure of the graphene Moiré and the extent of those regions. Depending on the rotation of the graphene lattice relative to the copper and the STM tip state, not all of the graphene regions reveal a strong Moiré pattern. (Imaging conditions for all images: $I = 6$nA, and $V = -0.2$ V).

coverage, as shown in **Figure 3**. In many ways, the growth of graphene on Cu(111) resembles a patchwork-like growth with many islands covering the surface with different orientations. It is possible to use differential conductance maps to examine the electrical properties of the graphene (**Figure 4**) and to see how the domain boundaries promote electron scattering and disrupt electrical continuity.[54,62] As the electrical properties of graphene are intimately connected with defects in the film, like domain boundaries, this study was important in indicating a major challenge in using Cu to grow high quality graphene. Finally, it was one of the first examples of graphene growth on a Cu single crystal.[54,78]

The STM studies of the graphene grown on Cu(111) prompted the first STM investigation of graphene on Cu foil as the early papers did not include a surface characterization with the resolution of STM.[55,79] One of the fascinating results from the STM studies of the graphene grown on polycrystalline Cu foil, beyond the resolution of the imaging itself, was the ability to probe the inert behavior of the graphene film in regards to both oxidation and thermal treatments.[55,61] The resolution of the imaging is facilitated by several large regions of single crystal domains. In **Figure 5**, it is evident how the areas of the sample which contain graphene remain impermeable to oxidation, which is clear in the corresponding differential conductance map, in direct opposition to those areas which are bare Cu and have subsequently become completely oxidized.[55] Performing XRD on the graphene areas showed that those areas were predominantly composed of the (100) facet, however, that is not a universal rule as both the (111) and (110) facets can also be formed in a majority on other samples. The rigidity of the sample extends beyond protection against oxidation. As shown in **Figure 6**, the graphene film can withstand a thermal treatment of 800 °C for 30 min. In the STM image, it is clear that the copper oxide has been removed with the high temperature treatment and clean Cu steps have been regained. Additionally, and most importantly, the graphene is maintained on the surface and is mostly unaltered with the possibility of some etching at the edges. These results emphatically reemphasize the special properties of graphene, especially its inert behavior and incredible stability, and how it could be used to protect metal surfaces from oxidation and degradation.[61]

Very recently, the CVD growth of graphene on plasmonic surfaces has been extended to include growth on Au foils and Au single crystals.[63–65] The presence of graphene was verified with Raman spectroscopy and the morphology was studied using SEM. Due to the similarities in the carbon solubility values between Cu and Au, 0.04% and 0.06% respectively, the authors hypothesized that the growth mechanism of graphene on the gold surface should be similar to copper, specifically that the mechanism is based on surface adsorption. In an effort to characterize the graphene on Au further, the graphene was transferred to insulating substrates to ultimately form field effect transistors for potential device applications.

CVD graphene growth on a wide variety of other, transition metal surfaces has been investigated thoroughly by a large number of research groups. On Ru(0001), graphene grows epitaxially across the surface over large lateral distances.[66] Furthermore, the layer, which is physisorbed to the underlying metal, is periodically rippled and shows inhomogeneities in charge distribution. Using both experimental and theoretical techniques, the presence of electron pockets at the peaks of the ripples was revealed; however, the exact origin of the corrugation remains controversial.[50] Considerable work on both the nature of the electronic interaction between the Ru substrate and the graphene and the quantification of the unit cell and superstructure has been conducted, but the full details go

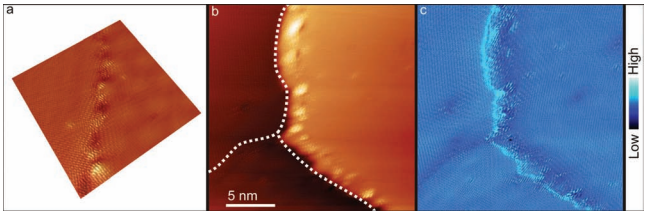

Figure 4. a) 3D rendering of an STM image focusing on a domain boundary in the graphene layer on Cu(111). b) Topographic STM image in which white dotted lines show both a Cu step edge and a domain boundary in the graphene film. It is also possible to see the electron scattering from the step edge in the image. c) Differential conductance image of the same area as (b), clearly indicating the electron scattering from the step edge and the domain boundary. These types of defects hinder the electrical properties of the epitaxial graphene grown on Cu(111).

beyond the scope of this review. The concept of a strongly corrugated graphene sheet extends to graphene grown on Rh(111). The different adsorptions sites of the carbon within the Moiré pattern of the only domain that is formed, causes different bonding and leads to a rippled surface structure.[67,68] Both theoretical and experimental evidence converge to agree on the existence of a buckled surface with the strongest adsorption occurring in the areas where the carbon atoms sit on the bridge sites of the underlying metallic layer.

In many ways similar to Ru, graphene growth on Ir(111) has been achieved via CVD growth, the structure of which exhibits a Moiré pattern due to the lattice mismatch between the Ir and graphene atomic distances.[69,80] Drawing on the fact that carbon is known to have a low solubility in Ir, the graphene grows in a self-limiting fashion. Importantly, it has been observed that graphene can grow up to two layers on the Ir surface, which indicates that some bulk segregation may also be occurring.[81] The epitaxial growth shows a preferred orientation with the atomic rows of the carbon aligning with the close-packed directions of the Ir atoms.[70,80,82] Unlike the Ru system, the Moiré structure on the Ir surface is less well-characterized with key surface studies not completed. Finally, like most graphene-transition metal systems, the level of interaction between the graphene and the Ir falls into the physisorbed realm with only local charge accumulation occurring at certain points in the superstructure.[83]

The weak interaction between the metal substrate and the graphene continues for the Pt(111) system, which leads to the formation of many rotational domains. The graphene can be formed in two ways either via bulk segregation or by CVD through the decomposition of hydrocarbons. According to both a theoretical model and experimental observations, the Moiré superstructures with a small mismatch are more energetically favorable and therefore occur with more frequency.[84] The situation for Pd(111) is unsurprisingly similar to that of Pt(111) with a weak interaction dominating and resulting in the creation of several rotational domains. There is some indication from STS studies that a 0.3 eV band gap may exist,[85] however, suggesting a strong hybridization, but further, global studies are needed to solidify this claim.

In contrast to some of the more recent studies of graphene on the plasmonic metals, graphene on Ni(111) has been studied

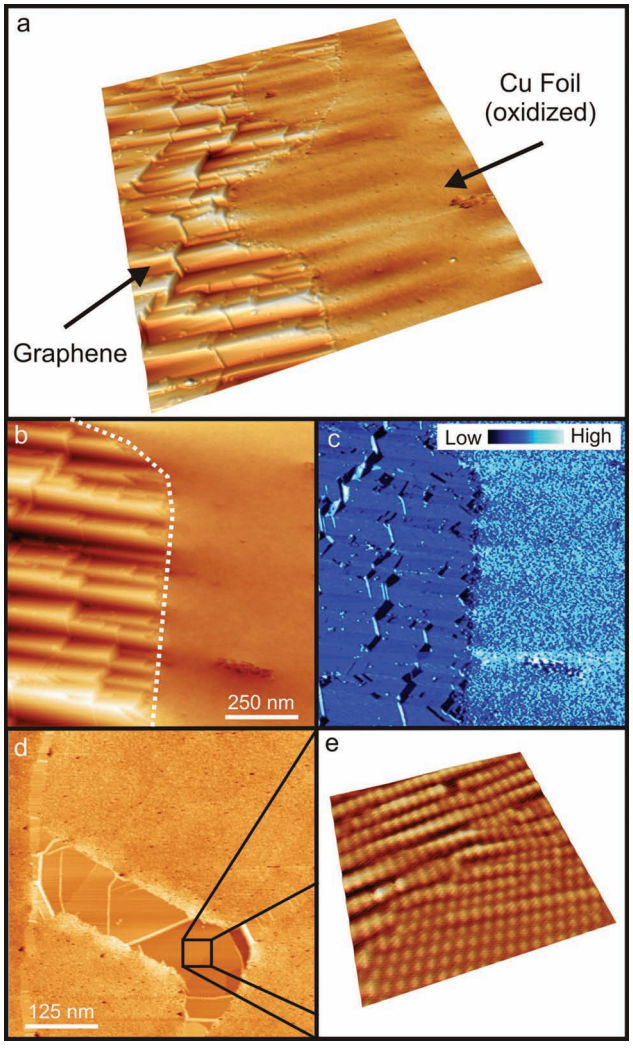

Figure 5. A compilation of STM images indicating the inertness of the graphene relative to oxidation. a) 3D STM image showing the results of an oxygen treatment. It is clear that the graphene film remains intact, while the area of bare metal becomes completely oxidized. b) Large-scale STM image focusing on the boundary between a graphene region and a cooper oxide region. c) The clear distinction between the two regions is emphasized in the *dI/dV* map of the same area, in which it is possible to see how the electronic behavior of the two areas differs due to their very different composition. d) Areas of clean graphene surrounded by large regions of oxidized copper can be observed in this topographic STM image. (e) Zoomed-in image of the area from the black box in (d) where it is possible to see the Moiré pattern of the graphene within that region. XRD studies indicate that this region is primarily composed of (100) facets. (Imaging conditions: (a-d): I = 100 pA, V = –1 V, I: I = 500 pA, –0.5 V).

since the early days of graphite research.[86] The early growth mode for graphene on Ni was carbon segregation from the bulk. Initially, it was believed that graphene on Ni only formed translational domains and not any rotational domains due to the close atomic lattice match between the two surfaces. Importantly, these translational domains have been verified with a variety of techniques including both DFT and STM. The STM studies showed how the non-equivalent atoms in the graphene

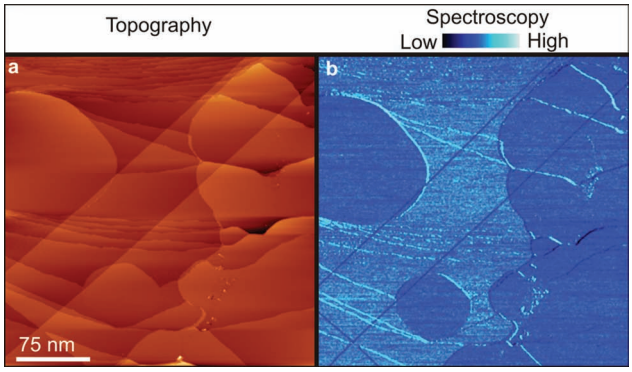

Figure 6. The continuous growth of graphene over atomic steps on Cu foil and the thermal stability of graphene is confirmed with STM imaging and spectroscopy. a) Topographic image of the graphene on Cu foil after an anneal to 800 °C for 30 min. The graphene clearly remains intact and continuous, while the heat has returned the copper to a metal state after removing the oxide layer. b) The maintenance of the graphene is verified with the differential conductance map, which is identical to graphene *dI/dV* signatures prior to the thermal treatment. (Imaging conditions: I = 100 pA, V = –0.6 V).

lattice appeared with a different contrast in the images.[87–89] Recently, rotational graphene domains with Moiré patterns have been shown to exist under specific growth conditions.[89,90] In terms of the electronic interaction between the graphene film and the Ni, ARPES studies indicate a strong interaction between the two.[91–93] Similarly, the story of graphene on Co(0001) closely resembles that of graphene on Ni(111) due to the fact that the lattice mismatch is only slightly larger in the case of Co.[94] STM images indicate that the graphene is commensurate with the underlying Ni and that non-equivalent, adjacent, carbon atoms exist within the graphene film. Finally, the electronic structure of the graphene on Co is quite analogous to that of graphene on Ni.

A somewhat missing piece of the graphene growth picture exists in regards to the growth on metal carbides, which have not been thoroughly studied since the discovery of graphene in explicit terms. Graphitic layers are known to exist on the top layer of metal carbides residing in the early transition metal series in the periodic table. The growth of graphene achieved through the exposure of these surfaces to ethylene in UHV appeared to be more easily achieved on the (111) plane rather than the (001) plane of the respective surfaces.[95–98] A revival of metal carbide science may be on the horizon due to the exponential growth of graphene research.

3. Processing and Modification

3.1. Transferring CVD Graphene

Once a graphene film is grown, it is sometimes necessary to transfer the graphene to an alternative substrate, such as an insulator which is required for most device applications,[49] and over time the process for graphene transfer has evolved substantially. Since the first "scotch tape transfer" by Geim and Novoselov, which ultimately led to a Nobel Prize, the transfer of single layer graphene has been performed using mechanical exfoliation.[1–3] The chemical reduction of exfoliated graphite oxide layers was also used to produce reduced graphene oxide platelets, but the electrical properties of such films were not sufficient.[99] Additionally, graphite has been partially exfoliated and then dispersed in a solvent; however, this technique produces a low yield and discontinuous films.[17,100] More recently in the work by Ruoff et al. on the CVD growth of graphene on Cu foil, the transfer of the film was accomplished through an etching process of the Cu foil and subsequent removal of the graphene film by various means as explained in detail below.[51] This method of graphene transfer has been perfected to result in the transfer of up to 30 inches of single layer graphene by a Korean team in 2010.[72]

Mechanical exfoliation is a technique which consists of the micro-mechanical alleviation of graphite, whereby graphene layers are removed from a graphite crystal with decreasing thickness; however, the largest graphene sheets made from this technique have only been ~1 mm^2 in surface area.[2,3,101] For applications purposes, such as the use graphene as a replacement for silicon in the current semiconductor industry, the large-scale transfer of graphene will be necessary. Although mechanical exfoliation is a relatively simple technique, it can be tedious and not very reliable as it yields randomly placed graphene sheets.

In a recently devised technique, single sheets of graphene were transferred from Cu foil to different substrates,[51,72] and later this process was extended to include graphene grown on other metallic foils.[18,47–49,77,102–104] In this case, the graphene is typically grown by the CVD method described in the previous section, after which the sample is placed in a solution of $FeNO_3$ that etches the Cu foil, leaving suspended graphene floating in the solution. The bare graphene film can then be transferred onto any substrate of choice with some exceptions. This process will not work for hydrophobic materials and requires all materials to be water resistant as it is a solution based technique. If this is not the case, the graphene can be transferred to a substrate using thermal release tape (Nitto Denko) which releases at temperatures between 90–120°C.[105] Recently, the thermal release tape was used to transfer 30 inches of graphene.[72] In examining the qualities of the transferred graphene, the sheet resistance has been shown to be as low as ~125 Ω with a 97.4% optical transmittance as well as a half-integer quantum hall effect, indicating the high quality of these films.[72] When stacked together, these films show superior qualities compared to current, commercial, transparent electrodes such as indium tin oxide. As such, these graphene films show great promises for the transparent electronics field with the hope of supplanting the current materials like indium and tin, which are becoming scarce. Although the etching and suspension technique has become quite reliable, it is not quite robust enough for the transfer of large-scale materials, where the thermal release tape has shown greater promise.[72]

Rather than removing the bare graphene film from the solution as described above, the graphene grown on the Cu foil can also be transferred using polydimethylsiloxane (PDMS) or polymethyl methalcrylate (PMMA) stamps to provide some film rigidity to the graphene layer.[18,47,51] Unfortunately, this transfer-printing method caused the graphene to form cracks

during the transfer, due to the nature of the mechanical properties of the graphene itself. In 2009, Ruoff et al. devised a process whereby once the PMMA/Gr sample is placed on a SiO_2/Si substrate, more PMMA is deposited and recurred.[49] The PMMA is then removed with acetone and the resulting film is of high quality.

3.2. H-Passivation for Bandgap Engineering

One of the biggest obstacles for graphene in the quest to supplant silicon in the multibillion dollar semiconductor industry is the fact that it is a gapless semiconductor, and thus, it cannot be directly used for digital electronics. As previously mentioned, various methods can be employed to open a band gap in graphene, including the quantum confinement of charges in graphene nanoribbons (GNRs) or through the chemical modification of graphene by either passivating it with atomic hydrogen or through solution chemistry. Hydrogen passivation of graphene affects the electronic properties of the film by converting it to a two-dimensional insulating material. Atomic hydrogen binds to the graphene, saturates the sp^2 bonds and converts them into sp^3 bonds which removes the conducting π-bands and opens an energy gap, subsequently leading to an insulating material known as graphane.[106–108]

In the case of hydrogen passivation, the graphene is grown on the Si face of a SiC(0001) sample after a cycle of high temperature flashes at 1250 °C as shown in **Figure 7**a. Once the graphene film is grown, the sample is annealed and exposed to a source of molecular hydrogen, which is cracked in a hot tungsten tube within a commercial, atomic hydrogen source. Hydrogen adsorption on epitaxial graphene leads to H-pair formation, which can have two configurations as schematically outlined in Figure 7b. Exposure to atomic hydrogen completely saturates the graphene surface (Figure 7b), however, hydrogen does not diffuse through the graphene monolayer or its edges, since the graphene is believed to be chemically bound to the SiC(0001)-$(6\sqrt{3} \times 6\sqrt{3})R30°$.[109,110] The passivation is also temperature dependent in the sense that below 400 °C passivation is observed, while above that temperature the hydrogen thermally desorbs. Furthermore, we have been able to use hydrogen passivation for nano-patterning the graphene grown on SiC, as well as for modifying the electronic properties and morphology using STM (Figure 7c–e).[111] The patterning process consists of "writing lines" on the surface via electron stimulated desorption. This is achieved by increasing the applied bias at a constant tip current; biases above +3.75 V desorb the hydrogen on the surface leaving pristine graphene areas, which recover their native electronic properties depending on the size of the pattern. In that same experiment, STS was used to study the local density of states of bilayer graphene grown on SiC which showed a dip in the spectra at –260 meV, as observed in Figure 7e. This observed dip is that of the shifted Dirac point relative to the Fermi level, which arises due to the graphene's interaction with the underlying surface states of the SiC.[111,112] The *dI/dV* measurement taken over the hydrogen-saturated surface shows a featureless spectrum with no sharp increases in the LDOS followed by a dip around the Dirac point, which indicates that hydrogen passivation does indeed affect the electronic structure of the graphene.

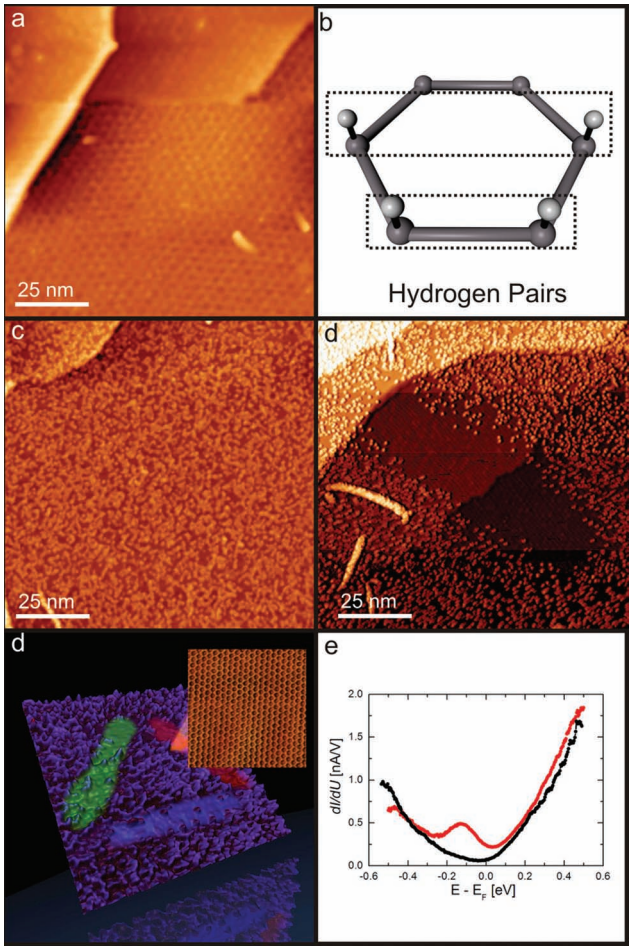

Figure 7. Hydrogen passivation of graphene on SiC. a) STM image showing a clean graphene surface, which was epitaxially grown on 4H:SiC(0001) (Imaging conditions: I = 0.1 nA, and V = 0.3 V). b) Schematic model of the lowest energy hydrogen pair configurations. c) Image showing a graphene surface fully saturated with hydrogen at room temperature (Imaging conditions: I = 0.1 nA, and V = 2 V). d) Topographic image showing a patterned area on the graphene. As the bias is increased to +4.5 V, the hydrogen easily desorbs from the surface in a controllable manner and leaves behind pristine graphene. It is also possible to pattern the graphene via this controllable desorption mechanism: the image shows the logo of Argonne National Laboratory. The inset shows the pristine graphene area, which is left behind after patterning. e) STS shows a characteristic dI/dV curve over clean, bilayer graphene (in red) with the Dirac point shifted from the Fermi level to a value of –260 meV, which is inherent to epitaxial graphene grown on SiC. This curve is overlaid with the *dI/dV* curve from a hydrogen passivated surface (black).

In addition to graphene grown on SiC, it is also possible to hydrogen passivate graphene grown on Cu foil, which is shown in **Figure 8**. The hydrogen does not adsorb on the bare Cu foil, most likely due to the presence of oxides on the exposed Cu area; however, the hydrogen does absorb on the areas of the surface covered with graphene (Figure 8a left). Once the graphene region is saturated with hydrogen, patterning could follow just as in the case of graphene on SiC (Figure 8a right). Importantly, each region of the surface (Cu foil, H on graphene on Cu, patterned graphene) has a clear signature in the *dI/dV* conductance map as indicated in Figure 8b.

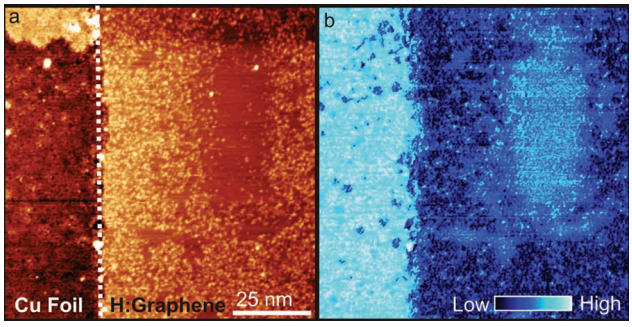

Figure 8. It is possible to hydrogen passivate graphene grown on Cu foil and to subsequently pattern it. a) STM image showing bare Cu foil (left) with an area of graphene that was hydrogen passivated (right) and subsequently patterned. b) Conductance map showing the same area as it appears with spectroscopy, where you can clearly see the difference in the local density of states between the two regions.

3.3. Molecular Self-Assembly on Graphene

In addition to the atomic passivation of surfaces, many surface studies are concentrated on the ability to decouple molecules from metallic substrates in an effort to isolate the molecule rather than probing a molecule-metal hybridized state. Recently Repp et al. used an insulating NaCl film to successfully decouple molecules from a metallic substrate, while still allowing a measurable tunneling current to pass through.[113] This molecular isolation ensured that the molecular orbitals of the pentacene molecules could be directly imaged and also allowed for bond information and geometry.[113–115] Graphene, a gapless material, also enables the study of non-hybridized molecules irrespective of the underlying substrate as it will essentially decouple the molecules, in a similar manner to the NaCl insulating layer. One of the first examples of molecular adsorption on graphene was the study of perylene-3,4,9,10-tetracarboxylic dianhydride (PTCDA) molecules which demonstrated the robust functionalization of graphene at room temperature.[116–118] Further molecular studies used graphene as a template for the study of Kagomé lattices with magnetic molecules.[119]

Recently, two studies of C_{60} molecules on graphene on Ru(0001)[120] and on SiC(0001)[121] were conducted in order to examine the molecule-surface interaction in graphene-based, organic photovoltaics. In the case of C_{60} on graphene/Ru(0001), the C_{60} molecules pack in a commensurate manner to form a supramolecular structure with a perfect and continuous periodicity with few defects. Even though it is reported that graphene decouples the C_{60} molecules from the underlying Ru, no study of the molecular orbitals or energetics were conducted.[120]

For the case of C_{60} on graphene/SiC(0001), the technological avenues are endless as the use of the underlying SiC makes the system readily available and transferrable to the current semiconductor industry. In this case, as in the case of C_{60}/graphene/Ru(0001), we found that the C_{60} molecules form a well-ordered, hexagonal, close-packed arrangement on the graphene surface as seen in **Figure 9**a–c, but they have no epitaxial relationship to the underlying substrate's orientation.[121] On the SiC reconstruction, the C_{60} molecules form superlattice patterns which are disordered in comparison to those on the graphene (Figure 9b,c). As was suggested by previous studies, the graphene essentially decouples the molecules from the surface, leading to a large HOMO-LUMO gap of 3.5 eV, which is shown in Figure 9d. This is the largest gap reported for C_{60} adsorbed to a substrate[122–125] and shows that graphene sufficiently shielded the C_{60} molecules from the substrate ensuring that there was very little charge transfer or any substrate-induced screening.

4. Conclusions

The focus of this article was to review some of the key advances in graphene synthesis, characterization, processing, and modification, while highlighting the role of the STM and its impact on each of these areas. However, specific attention was given to the various methods of large-scale synthesis, and the atomic-scale studies of graphene growth on single crystal Cu(111) and polycrystalline Cu foil. Processing and modification were discussed with an emphasis on graphene transfer, hydrogen passivation, and organic self-assembly. The STM is a powerful tool for characterizing hydrogen adsorption and the resulting modification of graphene's electronic properties and can also be used as a nano-patterning tool. This is by no means a thorough review of all graphene efforts, and the STM examples are specific to ongoing graphene research at the CNM.

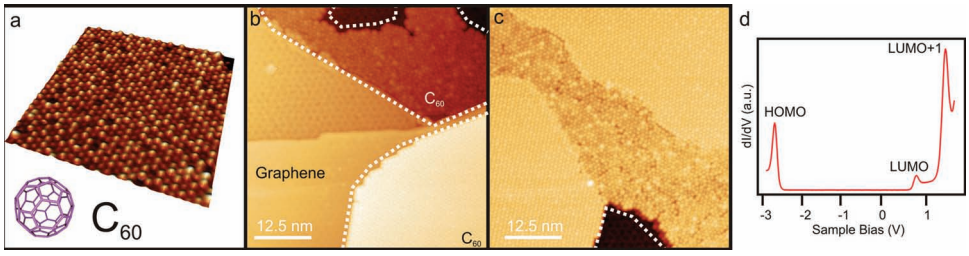

Figure 9. Molecular adsorption on graphene. a) STM image of C_{60} on graphene with a C_{60} fullerene molecular model aside. b) STM topographic images of the initial stages of growth of C_{60} molecules adsorbed on a submonolayer of epitaxial graphene on SiC with a structural assignment of the observed morphologies: single and bilayer graphene and C_{60} on graphene. c) Image of C_{60} covering areas of single layer, and bilayer graphene, as well as bare SiC. d) Representative *dI/dV* curve measured at 45 K on top of C_{60} molecules adsorbed onto monolayer graphene on SiC. All spectra were averaged over 180 individual spectra including forward and backward sweeps. The energetic positions of the HOMO-LUMO of C_{60} are indicated. (Imaging conditions for all images: $I = 1.5$ nA, and $V = 1.7$ V).

Acknowledgements

The use of the Center for Nanoscale Materials at Argonne National Laboratory was supported by the U.S. Department of Energy, Office of Science, Office of Basic Energy Sciences, under "SISGR" Contract No. DE-FG02-09ER16109 and Contract No. DE-AC02-06CH11357. This work is also supported by DARPA contract MIPR 10-E533.

Received: November 21, 2012
Published online: March 25, 2013

[1] K. S. Novoselov, A. K. Geim, S. V. Morozov, D. Jiang, Y. Zhang, S. V. Dubonos, I. V. Grigorieva, A. A. Firsov, *Science* **2004**, *306*, 666–669.
[2] K. S. Novoselov, D. Jiang, F. Schedin, T. J. Booth, V. V. Khotkevich, S. V. Morozov, A. K. Geim, *Proc. Nat. Acad. Sci. USA* **2005**, *102*, 10451–10453.
[3] K. S. Novoselov, A. K. Geim, S. V. Morozov, D. Jiang, M. I. Katsnelson, I. V. Grigorieva, S. V. Dubonos, A. A. Firsov, *Nature* **2005**, *438*, 197–200.
[4] A. K. Geim, K. S. Novoselov, *Nat. Mater.* **2007**, *6*, 183–191.
[5] A. H. C. Neto, F. Guinea, N. M. R. Peres, K. S. Novoselov, A. K. Geim, *Rev. Mod. Phys.* **2009**, *81*, 109–162.
[6] M. Y. Han, B. Oezyilmaz, Y. Zhang, P. Kim, *Phys. Rev. Lett.* **2007**, *98*, 206805.
[7] L. Jiao, L. Zhang, X. Wang, G. Diankov, H. Dai, *Nature* **2009**, *458*, 877–880.
[8] Y.-W. Son, M. L. Cohen, S. G. Louie, *Phys. Rev. Lett.* **2006**, *97*, 216806.
[9] D. V. Kosynkin, A. L. Higginbotham, A. Sinitskii, J. R. Lomeda, A. Dimiev, B. K. Price, J. M. Tour, *Nature* **2009**, *458*, 872–876.
[10] E. Bekyarova, M. E. Itkis, P. Ramesh, C. Berger, M. Sprinkle, W. A. de Heer, R. C. Haddon, *J. Amer. Chem. Soc.* **2009**, *131*, 1336–1337.
[11] T. O. Wehling, K. S. Novoselov, S. V. Morozov, E. E. Vdovin, M. I. Katsnelson, A. K. Geim, A. I. Lichtenstein, *Nano Lett.* **2008**, *8*, 173–177.
[12] A. A. Balandin, S. Ghosh, W. Bao, I. Calizo, D. Teweldebrhan, F. Miao, C. N. Lau, *Nano Lett.* **2008**, *8*, 902–907.
[13] J. Hu, X. Ruan, Y. P. Chen, *Nano Lett.* **2009**, *9*, 2730–2735.
[14] N. Phong, V. Berry, *J. Phys. Chem. Lett.* **2012**, *3*, 1024–1029.
[15] Y. Huang, X. Dong, Y. Shi, C. M. Li, L.-J. Li, P. Chen, *Nanoscale* **2010**, *2*, 1485–1488.
[16] Y. Dan, Y. Lu, N. J. Kybert, Z. Luo, A. T. C. Johnson, *Nano Lett.* **2009**, *9*, 1472–1475.
[17] P. Blake, P. D. Brimicombe, R. R. Nair, T. J. Booth, D. Jiang, F. Schedin, L. A. Ponomarenko, S. V. Morozov, H. F. Gleeson, E. W. Hill, A. K. Geim, K. S. Novoselov, *Nano Lett.* **2008**, *8*, 1704–1708.
[18] K. S. Kim, Y. Zhao, H. Jang, S. Y. Lee, J. M. Kim, K. S. Kim, J.-H. Ahn, P. Kim, J.-Y. Choi, B. H. Hong, *Nature* **2009**, *457*, 706–710.
[19] L. Qu, Y. Liu, J.-B. Baek, L. Dai, *ACS Nano* **2010**, *4*, 1321–1326.
[20] C. Xu, X. Wang, J. Zhu, *J. Phys. Chem. C* **2008**, *112*, 19841–19845.
[21] E. Yoo, J. Kim, E. Hosono, H.-s. Zhou, T. Kudo, I. Honma, *Nano Lett.* **2008**, *8*, 2277–2282.
[22] J. S. Bunch, A. M. van der Zande, S. S. Verbridge, I. W. Frank, D. M. Tanenbaum, J. M. Parpia, H. G. Craighead, P. L. McEuen, *Science* **2007**, *315*, 490–493.
[23] C. Chen, S. Rosenblatt, K. I. Bolotin, W. Kalb, P. Kim, I. Kymissis, H. L. Stormer, T. F. Heinz, J. Hone, *Nat. Nanotechnol.* **2009**, *4*, 861–867.
[24] J. M. Yuk, J. Park, P. Ercius, K. Kim, D. J. Hellebusch, M. F. Crommie, J. Y. Lee, A. Zettl, A. P. Alivisatos, *Science* **2012**, *336*, 61–64.
[25] C. Berger, Z. Song, X. Li, X. Wu, N. Brown, C. Naud, D. Mayou, T. Li, J. Hass, A. N. Marchenkov, E. H. Conrad, P. N. First, W. A. de Heer, *Science* **2006**, *312*, 1191–1196.
[26] G. M. Rutter, J. N. Crain, N. P. Guisinger, T. Li, P. N. First, J. A. Stroscio, *Science* **2007**, *317*, 219–222.
[27] V. W. Brar, Y. Zhang, Y. Yayon, T. Ohta, J. L. McChesney, A. Bostwick, E. Rotenberg, K. Horn, M. F. Crommie, *Appl. Phys. Lett.* **2007**, *91*, 122102–122103.
[28] E. Stolyarova, K. T. Rim, S. Ryu, J. Maultzsch, P. Kim, L. E. Brus, T. F. Heinz, M. S. Hybertsen, G. W. Flynn, *Proc. Nat. Acad. Sci.* **2007**, *104*, 9209–9212.
[29] A. J. Vanbommel, J. E. Crombeen, A. Vantooren, *Surf. Sci.* **1975**, *48*, 463–472.
[30] F. Owman, P. Martensson, *Surf. Sci.* **1995**, *330*, L639–L645.
[31] I. Forbeaux, J. M. Themlin, J. M. Debever, *Phys. Rev. B* **1998**, *58*, 16396–16406.
[32] L. Li, I. S. T. Tsong, *Surf. Sci.* **1996**, *351*, 141–148.
[33] L. Muehlhoff, W. J. Choyke, M. J. Bozack, J. T. Yates, *J. Appl. Phys.* **1986**, *60*, 2842–2853.
[34] I. Forbeaux, J. M. Themlin, J. M. Debever, *Surf. Sci.* **1999**, *442*, 9–18.
[35] I. Forbeaux, J. M. Themlin, A. Charrier, F. Thibaudau, J. M. Debever, *Appl. Surf. Sci.* **2000**, *162*, 406–412.
[36] T. Tsukamoto, M. Hirai, M. Kusaka, M. Iwami, T. Ozawa, T. Nagamura, T. Nakata, *Surf. Sci.* **1997**, *371*, 316–320.
[37] T. Tsukamoto, M. Hirai, M. Kusaka, M. Iwami, T. Ozawa, T. Nagamura, T. Nakata, *Appl. Surf. Sci.* **1997**, *113*, 467–471.
[38] X. N. Xie, R. Lim, J. Li, S. F. Y. Li, K. P. Loh, *Diam. Relat. Mater.* **2001**, *10*, 1218–1223.
[39] A. Charrier, A. Coati, T. Argunova, F. Thibaudau, Y. Garreau, R. Pinchaux, I. Forbeaux, J. M. Debever, M. Sauvage-Simkin, J. M. Themlin, *J. Appl. Phys.* **2002**, *92*, 2479–2484.
[40] T. Angot, M. Portail, I. Forbeaux, J. M. Layet, *Surf. Sci.* **2002**, *502*, 81–85.
[41] J. Hass, W. A. de Heer, E. H. Conrad, *J. Phys.: Condens. Matter* **2008**, *20*, 323202.
[42] K. Wakabayashi, M. Fujita, H. Ajiki, M. Sigrist, *Phys. Rev. B* **1999**, *59*, 8271–8282.
[43] M. L. Sadowski, G. Martinez, M. Potemski, C. Berger, W. A. de Heer, *Phys. Rev. Lett.* **2006**, *97*, 266405.
[44] C. Virojanadara, R. Yakimova, A. A. Zakharov, L. I. Johansson, *J. Phys. D Appl. Phys.* **2010**, *43*, 374010.
[45] F. Owman, P. Martensson, *Surf. Sci.* **1996**, *369*, 126–136.
[46] A. N. Obraztsov, E. A. Obraztsova, A. V. Tyurnina, A. A. Zolotukhin, *Carbon* **2007**, *45*, 2017–2021.
[47] A. Reina, X. Jia, J. Ho, D. Nezich, H. Son, V. Bulovic, M. S. Dresselhaus, J. Kong, *Nano Lett.* **2009**, *9*, 30–35.
[48] Q. Yu, J. Lian, S. Siriponglert, H. Li, Y. P. Chen, S.-S. Pei, *Appl. Phys. Lett.* **2008**, *93*, 113103.
[49] X. Li, Y. Zhu, W. Cai, M. Borysiak, B. Han, D. Chen, R. D. Piner, L. Colombo, R. S. Ruoff, *Nano Lett.* **2009**, *9*, 4359–4363.
[50] M. Batzill, *Surf. Sci. Rep.* **2012**, *67*, 83–115.
[51] X. Li, W. Cai, J. An, S. Kim, J. Nah, D. Yang, R. Piner, A. Velamakanni, I. Jung, E. Tutuc, S. K. Banerjee, L. Colombo, R. S. Ruoff, *Science* **2009**, *324*, 1312–1314.
[52] X. Li, W. Cai, L. Colombo, R. S. Ruoff, *Nano Lett.* **2009**, *9*, 4268–4272.
[53] X. Li, C. W. Magnuson, A. Venugopal, R. M. Tromp, J. B. Hannon, E. M. Vogel, L. Colombo, R. S. Ruoff, *J. Am. Chem. Soc.* **2011**, *133*, 2816–2819.
[54] L. Gao, J. R. Guest, N. P. Guisinger, *Nano Lett.* **2010**, *10*, 3512–3516.

[55] J. Cho, L. Gao, J. Tian, H. Cao, W. Wu, Q. Yu, E. N. Yitamben, B. Fisher, J. R. Guest, Y. P. Chen, N. P. Guisinger, *ACS Nano* **2011**, *5*, 3607–3613.
[56] L. Tao, J. Lee, H. Chou, M. Holt, R. S. Ruoff, D. Akinwande, *ACS Nano* **2012**, *6*, 2319–2325.
[57] Y. Ogawa, B. Hu, C. M. Orofeo, M. Tsuji, K.-i. Ikeda, S. Mizuno, H. Hibino, H. Ago, *J. Phys. Chem. Lett.* **2012**, *3*, 219–226.
[58] S. Nie, J. M. Wofford, N. C. Bartelt, O. D. Dubon, K. F. McCarty, *Phys. Rev. B* **2011**, *84*, 155425.
[59] K. M. Reddy, A. D. Gledhill, C.-H. Chen, J. M. Drexler, N. P. Padture, *Appl. Phys. Lett.* **2011**, *98*, 113117.
[60] P. A. Khomyakov, G. Giovannetti, P. C. Rusu, G. Brocks, J. van den Brink, P. J. Kelly, *Phys. Rev. B* **2009**, *79*, 195425.
[61] S. Chen, L. Brown, M. Levendorf, W. Cai, S.-Y. Ju, J. Edgeworth, X. Li, C. W. Magnuson, A. Velamakanni, R. D. Piner, J. Kang, J. Park, R. S. Ruoff, *ACS Nano* **2011**, *5*, 1321–1327.
[62] J. Tian, H. Cao, W. Wu, Q. Yu, Y. P. Chen, *Nano Lett.* **2011**, *11*, 3663–3668.
[63] T. Oznuluer, E. Pince, E. O. Polat, O. Balci, O. Salihoglu, C. Kocabas, *Appl. Phys. Lett.* **2011**, *98*, 183101.
[64] J. M. Wofford, E. Starodub, A. L. Walter, S. Nie, A. Bostwick, N. C. Bartelt, K. Thuermer, E. Rotenberg, K. F. McCarty, O. D. Dubon, *New J. Chem.* **2012**, *14*.
[65] S. Nie, N. C. Bartelt, J. M. Wofford, O. D. Dubon, K. F. McCarty, K. Thuermer, *Phys. Rev. B* **2012**, *85*, 205406.
[66] A. L. Vazquez de Parga, F. Calleja, B. Borca, M. C. G. Passeggi Jr., J. J. Hinarejos, F. Guinea, R. Miranda, *Phys. Rev. Lett.* **2008**, *100*, 056807.
[67] A. B. Preobrajenski, M. L. Ng, A. S. Vinogradov, N. Martensson, *Phys. Rev. B* **2008**, *78*, 073401.
[68] C. Enderlein, Y. S. Kim, A. Bostwick, E. Rotenberg, K. Horn, *New J. Chem.* **2010**, *12*, 033014.
[69] J. Coraux, A. T. N'Diaye, C. Busse, T. Michely, *Nano Lett.* **2008**, *8*, 565–570.
[70] E. Loginova, S. Nie, K. Thuermer, N. C. Bartelt, K. F. McCarty, *Phys. Rev. B* **2009**, *80*, 085430.
[71] P. Y. Huang, C. S. Ruiz-Vargas, A. M. van der Zande, W. S. Whitney, M. P. Levendorf, J. W. Kevek, S. Garg, J. S. Alden, C. J. Hustedt, Y. Zhu, J. Park, P. L. McEuen, D. A. Muller, *Nature* **2011**, *469*, 389–392.
[72] S. Bae, H. Kim, Y. Lee, X. Xu, J.-S. Park, Y. Zheng, J. Balakrishnan, T. Lei, H. R. Kim, Y. I. Song, Y.-J. Kim, K. S. Kim, B. Ozyilmaz, J.-H. Ahn, B. H. Hong, S. Iijima, *Nat. Nanotechnol.* **2010**, *5*, 574–578.
[73] H. Cao, Q. Yu, L. A. Jauregui, J. Tian, W. Wu, Z. Liu, R. Jalilian, D. K. Benjamin, Z. Jiang, J. Bao, S. S. Pei, Y. P. Chen, *Appl. Phys. Lett.* **2010**, *96*, 122106.
[74] A. Venugopal, J. Chan, X. Li, C. W. Magnuson, W. P. Kirk, L. Colombo, R. S. Ruoff, E. M. Vogel, *J. Appl. Phys.* **2011**, *109*, 104511.
[75] X. Li, C. W. Magnuson, A. Venugopal, J. An, J. W. Suk, B. Han, M. Borysiak, W. Cai, A. Velamakanni, Y. Zhu, L. Fu, E. M. Vogel, E. Voelkl, L. Colombo, R. S. Ruoff, *Nano Lett.* **2010**, *10*, 4328–4334.
[76] J. An, E. Voelkl, J. W. Suk, X. Li, C. W. Magnuson, L. Fu, P. Tiemeijer, M. Bischoff, B. Freitag, E. Popova, R. S. Ruoff, *ACS Nano* **2011**, *5*, 2433–2439.
[77] M. P. Levendorf, C. S. Ruiz-Vargas, S. Garg, J. Park, *Nano Lett.* **2009**, *9*, 4479–4483.
[78] H. I. Rasool, E. B. Song, M. Mecklenburg, B. C. Regan, K. L. Wang, B. H. Weiller, J. K. Gimzewski, *J. Am. Chem. Soc.* **2011**, *133*, 12536–12543.
[79] H. I. Rasool, E. B. Song, M. J. Allen, J. K. Wassei, R. B. Kaner, K. L. Wang, B. H. Weiller, J. K. Gimzewski, *Nano Lett.* **2011**, *11*, 251–256.
[80] A. T. N'Diaye, J. Coraux, T. N. Plasa, C. Busse, T. Michely, *New J. Chem.* **2008**, *10*, 043033.
[81] S. Nie, A. L. Walter, N. C. Bartelt, E. Starodub, A. Bostwick, E. Rotenberg, K. F. McCarty, *ACS Nano* **2011**, *5*, 2298–2306.
[82] J. Coraux, A. T. N'Diaye, M. Engler, C. Busse, D. Wall, N. Buckanie, F.-j. M. Z. Heringdorf, R. van Gastel, B. Poelsema, T. Michely, *New J. Chem.* **2009**, *11*, 023006.
[83] C. Busse, P. Lazic, R. Djemour, J. Coraux, T. Gerber, N. Atodiresei, V. Caciuc, R. Brako, A. T. N'Diaye, S. Bluegel, J. Zegenhagen, T. Michely, *Phys. Rev. Lett.* **2011**, *107*, 036101.
[84] P. Merino, M. Svec, A. L. Pinardi, G. Otero, J. A. Martin-Gago, *ACS Nano* **2011**, *5*, 5627–5634.
[85] S.-Y. Kwon, C. V. Ciobanu, V. Petrova, V. B. Shenoy, J. Bareno, V. Gambin, I. Petrov, S. Kodambaka, *Nano Lett.* **2009**, *9*, 3985–3990.
[86] F. J. Derbyshire, A. E. B. Presland, D. L. Trimm, *Carbon* **1975**, *13*, 111–113.
[87] J. Lahiri, T. S. Miller, A. J. Ross, L. Adamska, I. I. Oleynik, M. Batzill, *New J. Chem.* **2011**, *13*, 025001.
[88] J. Lahiri, Y. Lin, P. Bozkurt, I. I. Oleynik, M. Batzill, *Nat. Nanotechnol.* **2010**, *5*, 326–329.
[89] Y. S. Dedkov, M. Fonin, *New J. Chem.* **2010**, *12*, 125004.
[90] J. Lahiri, T. Miller, L. Adamska, I. I. Oleynik, M. Batzill, *Nano Lett.* **2011**, *11*, 518–522.
[91] A. Nagashima, N. Tejima, C. Oshima, *Phys. Rev. B* **1994**, *50*, 17487–17495.
[92] Y. S. Dedkov, M. Fonin, U. Ruediger, C. Laubschat, *Phys. Rev. Lett.* **2008**, *100*, 107602.
[93] A. Varykhalov, J. Sanchez-Barriga, A. M. Shikin, C. Biswas, E. Vescovo, A. Rybkin, D. Marchenko, O. Rader, *Phys. Rev. Lett.* **2008**, *101*, 157601.
[94] D. Eom, D. Prezzi, K. T. Rim, H. Zhou, M. Lefenfeld, S. Xiao, C. Nuckolls, M. S. Hybertsen, T. F. Heinz, G. W. Flynn, *Nano Lett.* **2009**, *9*, 2844–2848.
[95] P. M. Stefan, M. L. Shek, I. Lindau, W. E. Spicer, L. I. Johansson, F. Herman, R. V. Kasowski, G. Brogen, *Phys. Rev. B* **1984**, *29*, 5423–5444.
[96] T. Aizawa, R. Souda, S. Otani, Y. Ishizawa, C. Oshima, *Phys. Rev. B* **1990**, *42*, 11469–11478.
[97] T. Aizawa, R. Souda, S. Otani, Y. Ishizawa, C. Oshima, *Phys. Rev. Lett.* **1990**, *64*, 768–771.
[98] A. Nagashima, K. Nuka, K. Satoh, H. Itoh, T. Ichinokawa, C. Oshima, S. Otani, *Surf. Sci.* **1993**, *287*, 609–613.
[99] S. Park, R. S. Ruoff, *Nat. Nanotechnol.* **2009**, *4*, 217–224.
[100] Y. Hernandez, V. Nicolosi, M. Lotya, F. M. Blighe, Z. Sun, S. De, I. T. McGovern, B. Holland, M. Byrne, Y. K. Gun'ko, J. J. Boland, P. Niraj, G. Duesberg, S. Krishnamurthy, R. Goodhue, J. Hutchison, V. Scardaci, A. C. Ferrari, J. N. Coleman, *Nat. Nanotechnol.* **2008**, *3*, 563–568.
[101] Y. B. Zhang, Y. W. Tan, H. L. Stormer, P. Kim, *Nature* **2005**, *438*, 201–204.
[102] L. Song, L. Ci, W. Gao, P. M. Ajayan, *ACS Nano* **2009**, *3*, 1353–1356.
[103] Z.-Y. Juang, C.-Y. Wu, A.-Y. Lu, C.-Y. Su, K.-C. Leou, F.-R. Chen, C.-H. Tsai, *Carbon* **2010**, *48*, 3169–3174.
[104] Y. Lee, S. Bae, H. Jang, S. Jang, S.-E. Zhu, S. H. Sim, Y. I. Song, B. H. Hong, J.-H. Ahn, *Nano Lett.* **2010**, *10*, 490–493.
[105] Nitto Denko America, Inc. 48500 Fremont Blvd., Fremont, CA 92058, USA.
[106] M. H. F. Sluiter, Y. Kawazoe, *Phys. Rev. B* **2003**, *68*, 085410.
[107] J. O. Sofo, A. S. Chaudhari, G. D. Barber, *Phys. Rev. B* **2007**, *75*, 153401.
[108] D. C. Elias, R. R. Nair, T. M. G. Mohiuddin, S. V. Morozov, P. Blake, M. P. Halsall, A. C. Ferrari, D. W. Boukhvalov, M. I. Katsnelson, A. K. Geim, K. S. Novoselov, *Science* **2009**, *323*, 610–613.

[109] N. P. Guisinger, G. M. Rutter, J. N. Crain, P. N. First, J. A. Stroscio, *Nano Lett.* **2009**, *9*, 1462–1466.
[110] C. Riedl, C. Coletti, T. Iwasaki, A. A. Zakharov, U. Starke, *Phys. Rev. Lett.* **2009**, *103*, 246804.
[111] P. Sessi, J. R. Guest, M. Bode, N. P. Guisinger, *Nano Lett.* **2009**, *9*, 4343–4347.
[112] T. Ohta, A. Bostwick, T. Seyller, K. Horn, E. Rotenberg, *Science* **2006**, *313*, 951–954.
[113] J. Repp, G. Meyer, S. M. Stojkovic, A. Gourdon, C. Joachim, *Phys. Rev. Lett.* **2005**, *94*, 026803.
[114] J. Repp, G. Meyer, S. Paavilainen, F. E. Olsson, M. Persson, *Science* **2006**, *312*, 1196–1199.
[115] P. Liljeroth, I. Swart, S. Paavilainen, J. Repp, G. Meyer, *Nano Lett.* **2010**, *10*, 2475–2479.
[116] Q. H. Wang, M. C. Hersam, *Nat. Chem.* **2009**, *1*, 206–211.
[117] P. Lauffer, K. V. Emtsev, R. Graupner, T. Seyller, L. Ley, *Phys. Stat. Solidi B* **2008**, *245*, 2064.
[118] H. Huang, S. Chen, X. Gao, W. Chen, A. T. S. Wee, *ACS Nano* **2009**, *3*, 3431–3436.
[119] J. Mao, H. Zhang, Y. Jiang, Y. Pan, M. Gao, W. Xiao, H. J. Gao, *J. Am. Chem. Soc.* **2009**, *131*, 14136–14137.
[120] G. Li, H. T. Zhou, L. D. Pan, Y. Zhang, J. H. Mao, Q. Zou, H. M. Guo, Y. L. Wang, S. X. Du, H. J. Gao, *Appl. Phys. Lett.* **2012**, *100*, 013304.
[121] J. Cho, J. Smerdon, L. Gao, O. Suezer, J. R. Guest, N. P. Guisinger, *Nano Lett.* **2012**, *12*, 3018–3024.
[122] T. R. Ohno, Y. Chen, S. E. Harvey, G. H. Kroll, J. H. Weaver, R. E. Haufler, R. E. Smalley, *Phys. Rev. B* **1991**, *44*, 13747–13755.
[123] R. Hesper, L. H. Tjeng, G. A. Sawatzky, *Europhys. Lett.* **1997**, *40*, 177–182.
[124] M. Grobis, X. Lu, M. F. Crommie, *Phys. Rev. B* **2002**, *66*, 161408.
[125] G. Schull, N. Neel, M. Becker, J. Kroeger, R. Berndt, *New J. Chem.* **2008**, *10*, 065012.